J|A|C|S ARTICLES

Published on Web 01/02/2009

Probing General Acid Catalysis in the Hammerhead Ribozyme

Jason M. Thomas and David M. Perrin*

Department of Chemistry, University of British Columbia, 2036 Main Mall, Vancouver, B.C., Canada, V6T 1Z1

Received October 2, 2008; E-mail: dperrin@chem.ubc.ca

Abstract: Recent crystallographic and computational studies have provided fresh insights into the catalytic mechanism of the RNA-cleaving hammerhead ribozyme. Based on these findings, specific ribozyme functional groups have been hypothesized to act directly as the general acid and base catalysts, although the catalytic role of divalent metal cations (M^{2+}) remains uncertain. We now report a functional characterization of the general acid catalysis mechanism and the role of an M^{2+} cofactor therein, for the *S. mansoni* hammerhead (an "extended" hammerhead ribozyme). We have compared hammerhead cleavage of substrates with natural (ribo-phosphodiester) versus bridging-5′-phosphorothioate scissile linkages, in the contexts of active site mutations and M^{2+} substitution. Cleavage of the natural substrate is inhibited by modification of the G8 2′-OH ribozyme residue and depends strongly upon the presence and identity of an M^{2+} cofactor; in contrast, cleavage of the bridging-phosphorothioate substrate is conspicuously insensitive to any of these factors. These results imply that (1) both an M^{2+} cofactor and the G8 2′-OH play crucial roles in hammerhead general acid catalysis and (2) the M^{2+} cofactor does not contribute to general acid catalysis via Lewis acid stabilization of the leaving group. General acid pK_a perturbation was also demonstrated for both M^{2+} substitution and G8 2′-OH modification, which suggests transition state M^{2+} coordination of the G8 2′-OH, to lower its pK_a and improve its ability to transfer a proton to the leaving group. We also report a simple method for synthesizing radiolabeled bridging-5′-phosphorothioate substrates.

Introduction

Until recently, a detailed understanding of the active site structure and catalytic mechanism of the RNA-cleaving hammerhead ribozyme had been elusive. The results of *in vitro* activity studies clearly contradicted early crystal structures[1−3] of "minimal" hammerhead ribozymes;[4,5] although informative, these structures are now believed to represent a pervasive yet inactive ribozyme conformation.[6,7] The more recently characterized "extended" hammerhead ribozymes, such as the *S. mansoni* sequence, exhibit greatly enhanced catalysis at lower divalent metal (M^{2+}) concentrations.[8−10] These extended hammerheads benefit from additional tertiary stabilization of their active conformation provided by natural peripheral sequence regions, which had been deleted in the standard minimal hammerheads (Figure 1). Recent crystal structures[11−13] of extended hammerhead ribozymes differ radically from those of minimal hammerhead ribozymes and have provided novel insight into hammerhead structure and catalysis. Much of the earlier biochemical data can now be reconciled with the extended hammerhead crystal structures; therefore, these structures are believed to closely represent the catalytically active ribozyme conformation.[6,7] In light of the extended hammerhead structures, a novel mechanistic hypothesis involving ribozyme mediated general acid/base catalysis has been proposed (Scheme 1).[11] Functional studies have confirmed quite convincingly that G12 acts as a general base;[14,15] however, the mechanism of general acid catalysis and the role of an M^{2+} cofactor (if any) in catalysis both require clarification and are the focus of this study.

(1) Pley, H. W.; Flaherty, K. M.; McKay, D. B. *Nature* **1994**, *372*, 68–74.
(2) Scott, W. G.; Finch, J. T.; Klug, A. *Cell* **1995**, *81*, 991–1002.
(3) Scott, W. G.; Murray, J. B.; Arnold, J. R.; Stoddard, B. L.; Klug, A. *Science* **1996**, *274*, 2065–2069.
(4) Blount, K. F.; Uhlenbeck, O. C. *Annu. Rev. Biophys. Biomol. Struct.* **2005**, *34*, 415–440.
(5) In particular, the work of Burke and coworkers should be noted as a clear illustration of the discrepancy between the results of functional experiments and minimal hammerhead crystal structures. Their findings correctly predicted the proximity of several ribozyme residues to the substrate cleavage site, as observed later in the *S. mansoni* crystal structure. See: (a) Heckman, J. E.; Lambert, D.; Burke, J. M. *Biochemistry* **2005**, *44*, 4148–4156. (b) Lambert, D.; Heckman, J. E.; Burke, J. M. *Biochemistry* **2006**, *45*, 7140–7147. (c) Han, J.; Burke, J. M. *Biochemistry* **2005**, *44*, 7864–7870.
(6) Nelson, J. A.; Uhlenbeck, O. C. *Mol. Cell* **2006**, *23*, 447–450.
(7) Nelson, J. A.; Uhlenbeck, O. C. *RNA* **2008**, *14*, 605–615.
(8) Khvorova, A.; Lescoute, A.; Westhof, E.; Jayasena, S. D. *Nat. Struct. Biol.* **2003**, *10*, 708–712.
(9) Canny, M. D.; Jucker, F. M.; Kellogg, E.; Khvorova, A.; Jayasena, S. D.; Pardi, A. *J. Am. Chem. Soc.* **2004**, *126*, 10848–10849.
(10) Saksmerprome, V.; Roychowdhury-Saha, M.; Jayasena, S. D.; Khvorova, A.; Burke, D. H. *RNA* **2004**, *10*, 1916–1924.
(11) Martick, M.; Scott, W. G. *Cell* **2006**, *126*, 309–320.
(12) Martick, M.; Lee, T.-S.; York, D. M.; Scott, W. G. *Chem. Biol.* **2008**, *15*, 332–342.
(13) Chi, Y.-I.; Martick, M.; Lares, M.; Kim, R.; Scott, W. G.; Kim, S.-H. *PLoS Biol.* **2008**, *6*, e234.
(14) Thomas, J. M.; Perrin, D. M. *J. Am. Chem. Soc.* **2008**, *130*, 15467–15675.
(15) Han, J.; Burke, J. M. *Biochemistry* **2005**, *44*, 7864–7870.
(16) Hertel, K. J.; Herschlag, D. J. A.; Uhlenbeck, O. C. *Biochemistry* **1994**, *33*, 3374–3385.
(17) Lee, T.-S.; Lopez, C. S.; Giambasu, G. M.; Martick, M.; Scott, W. G.; York, D. M. *J. Am. Chem. Soc.* **2008**, *130*, 3053–3064.
(18) Lee, T.-S.; Silva-Lopez, C.; Martick, M.; Scott, W. G.; York, D. M. *J. Chem. Theory Comput.* **2007**, *3*, 325–327.

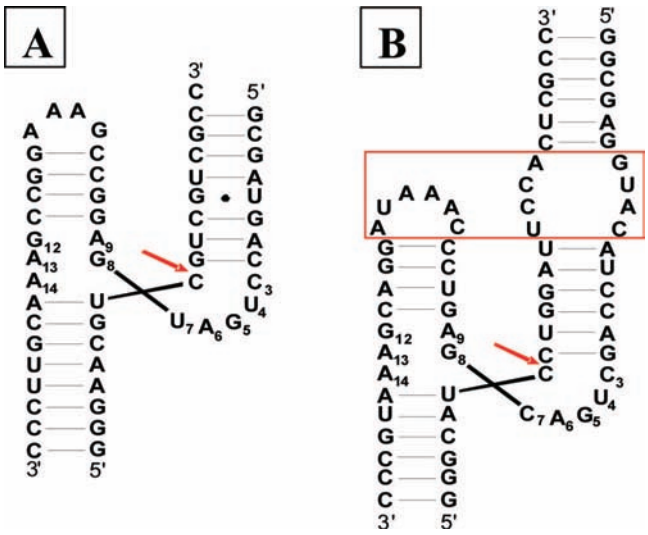

Figure 1. Secondary structure representations of (A) the HH16 minimal[16] and (B) the *S. mansoni* extended[9] hammerhead ribozymes. Red arrows indicate the substrate cleavage sites and the nucleotides in the conserved catalytic core are numbered according to convention. The additional tertiary interaction present in the extended hammerhead is highlighted by the red box.

Scheme 1. Hypothetical Catalytic Mechanism of the Hammerhead Ribozyme[a]

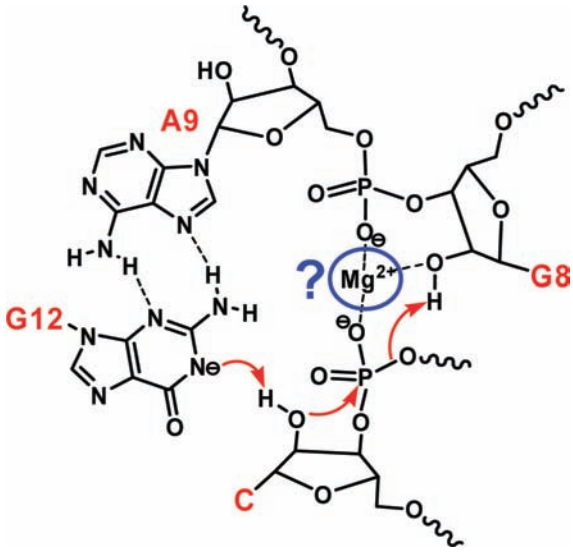

[a] Based on the *S. mansoni* hammerhead crystal structure and subsequent computational analysis, where G12 acts as general base and the G8 2′-OH acts as general acid with possible Mg^{2+}-assistance.[11−13,17,18]

The role of the M^{2+} has been the subject of considerable scrutiny in earlier biochemical and spectroscopic experiments. Although reasonable catalytic activity was observed in high concentrations of monovalent cations alone,[19,20] an M^{2+} cofactor appeared to play an important role in catalysis. Based on the results of nonbridging phosphorothioate substitution experiments, an M^{2+} cofactor was proposed to stabilize the transition state by bridging the *pro*-R oxygens of the A9 and scissile phosphates of the ribozyme and substrate strands, respectively.[21−26] In contrast to the minimal hammerhead structures,[27] the extended hammerhead crystal structures now confirm that the A9 phosphate binds an M^{2+} cofactor close to the active site, although no bonding interaction with the scissile phosphate or the putative general acid (the G8 2′-OH) was observed.[12,13] Also of particular note, Burke and co-workers have demonstrated that substitution of Cd^{2+} for Mg^{2+} leads to a drastic change in the pH−rate profile of the RzB extended hammerhead.[28] This effect could be consistent with general acid catalysis by either an M^{2+}-bound water molecule or an M^{2+}-bound ribozyme functional group (such as the G8 2′-OH); that is, M^{2+} substitution could cause pK_a perturbation in either case.

Based on the extended hammerhead crystal structures, significant computational effort has also been devoted to predicting the role of an M^{2+} cofactor in transition state stabilization. York and co-workers suggest that an M^{2+} cofactor bound to the A9 phosphate could stabilize the buildup of negative charge on the nonbridging oxygens of the scissile phosphate, as well as coordinate the G8 2′-OH to lower its pK_a and facilitate general acid catalysis (Scheme 1).[12,17,18]

In this study, we provide experimental evidence based on chemical probing and *in vitro* kinetic analysis to identify the role of ribozyme functional groups and an M^{2+} cofactor in general acid catalysis. To this end, we have investigated hammerhead cleavage of a bridging phosphorothioate ("S-link") substrate, as this approach has proven useful for probing general acid catalysis in other phosphodiester cleavage catalysts.[29−37] In contrast to the native oxygen leaving group, the departure of the sulfur leaving group is not readily assisted by Brønsted acid catalysis[29,38] because (a) the sulfur atom in the P−S thioether-like bond is a poor hydrogen-bond acceptor; (b) the thiolate, as a leaving group, has a much lower pK_a and is thus more stable than the alkoxide leaving group; and (c) the P−S bond is more labile than the native P−O bond due to a lower bond dissociation

(19) Murray, J. B.; Seyhan, A. A.; Walter, N. G.; Burke, J. M.; Scott, W. G. *Chem. Biol.* **1998**, *5*, 587–595.
(20) Curtis, E. A.; Bartel, D. P. *RNA* **2001**, *7*, 546–552.
(21) Peracchi, A.; Beigelman, L.; Scott, E. C.; Uhlenbeck, O. C.; Herschlag, D. *J. Biol. Chem.* **1997**, *272*, 26822–26826.
(22) Wang, S.; Karbstein, K.; Peracchi, A.; Beigelman, L.; Herschlag, D. *Biochemistry* **1999**, *38*, 14363–14378.
(23) Maderia, M.; Hunsicker, L. M.; DeRose, V. J. *Biochemistry* **2000**, *39*, 12113–12120.
(24) Suzumura, K.; Yoshinari, K.; Tanaka, Y.; Takagi, Y.; Kasai, Y.; Warashina, M.; Kuwabara, T.; Orita, M.; Taira, K. *J. Am. Chem. Soc.* **2002**, *124*, 8230–8236.
(25) Cunningham, L. A.; Li, J.; Lu, Y. *J. Am. Chem. Soc.* **1998**, *120*, 4518–4519.
(26) Osborne, E. M.; Schaak, J. E.; Derose, V. J. *RNA* **2005**, *11*, 187–196.
(27) Murray, J. B.; Scott, W. G. *J. Mol. Biol.* **1999**, *296*, 33–41.
(28) Roychowdhury-Saha, M.; Burke, D. H. *RNA* **2006**, *12*, 1846–1852.
(29) Das, S. R.; Piccirilli, J. A. *Nat. Chem. Biol.* **2005**, *1*, 45–52.
(30) Krogh, B. O.; Shuman, S. *Mol. Cell* **2000**, *5*, 1035–1041.
(31) Piccirilli, J. A.; Vyle, J. S.; Caruthers, M. H.; Cech, T. R. *Nature* **1993**, *361*, 85–88.
(32) Kuimelis, R. G.; McLaughlin, L. W. *J. Am. Chem. Soc.* **1995**, *117*, 11019–11020.
(33) Zhou, D.-M.; Usman, N.; Wincott, F. E.; Matulic-Adamic, J.; Orita, M.; Zhang, L.-H.; Komiyama, M.; Kumar, P. K. R.; Taira, K. *J. Am. Chem. Soc.* **1996**, *118*, 5862–5866.
(34) An analogous experiment, which substituted a low pK_a nitrophenolate leaving group in place of the native alkoxide, has been reported to confirm that His119 performs general acid catalysis in RNaseA catalysis of RNA cleavage. See: Thompson, J. E.; Raines, R. T. *J. Am. Chem. Soc.* **1994**, *116*, 5467–5468.
(35) Hondal, R. J.; Bruzik, K. S.; Zhao, Z.; Tsai, M.-D. *J. Am. Chem. Soc.* **1997**, *119*, 5477–5478.
(36) Hondal, R. J.; Zhao, Z.; Riddle, S. R.; Kravchuk, A. V.; Liao, H.; Bruzik, K. S.; Tsai, M.-D. *J. Am. Chem. Soc.* **1997**, *119*, 9933–9934.
(37) Kubiak, R. J.; Hondal, R. J.; Yue, X.; Tsai, M.-D.; Bruzik, K. S. *J. Am. Chem. Soc.* **1999**, *121*, 488–489.
(38) Thomson, J. B.; Patel, B. K.; Jimenez, V.; Eckart, K.; Eckstein, F. *J. Org. Chem.* **1996**, *61*, 6273–6281.

energy. Consequently, active site mutations or reaction conditions which specifically disrupt general acid catalysis severely impair cleavage of the native ("O-link") substrate but should not significantly affect cleavage of the S-link substrate.[29,35−37] Lewis acid stabilization of the leaving group by an M^{2+} cofactor can also be revealed using S-link substrates. For example, direct M^{2+} coordination of the leaving group was revealed in the *Tetrahymena* ribozyme by the specific activation of S-link cleavage by soft metal cations.[31]

The results presented herein for S-link substrate cleavage by the *S. mansoni* hammerhead appear to rule out Lewis acid catalysis by an M^{2+} cofactor. Instead, our results suggest that an M^{2+} cofactor serves to facilitate proton transfer from the G8 2′-OH to the leaving group, consistent with recent computational predictions.[17] This conclusion is supported by our observations that (1) when Mg^{2+} is replaced with Cd^{2+} the general acid pK_a is perturbed downward, and (2) when proton transfer from the G8 2′-OH is interrupted (in the dG8 and 2′-OMe-G8 variants) the general acid pK_a is perturbed upward. We hypothesize that the latter effect is attributable to a higher pK_a of an M^{2+}-bound water molecule acting as a proxy general acid in the absence of the G8 2′-OH (water has a higher pK_a than the 2′-OH in RNA[39−41]). Our data also indicate that active site structural interactions, which were newly revealed in the extended hammerhead crystal structures, are crucial for efficient general acid catalysis.

Materials and Methods

Chemicals and Biochemicals. All chemicals and buffers salts were purchased from Sigma-Aldrich. DNA and RNA oligonucleotides were synthesized by the University of Calgary DNA Services Laboratory. RNA was also synthesized by *in vitro* transcription from synthetic DNA templates[42] using the T7 Mega Short Script kit (Ambion). T4 polynucleotide kinase and T4 DNA ligase were purchased from Invitrogen, RNase A was purchased from Fermentas, Superase-in RNase inhibitor was from Ambion, γ-^{32}P-ATP was from Perkin-Elmer, and streptavidin magnetic particles were from Roche.

Oligonucleotide Sequences. The *S. mansoni* hammerhead ribozyme and substrate sequences were taken from Canny et al.[9] WT ribozyme sequence 5′-GGCGAGGUACAUCCAGCUGACGAGUCCCAAAUAGGACGAAAUGCCC (mutations made to this sequence are described in the text); 5′-product (**1**): 5′-d(GGGCAT)**X** where **X** is ribo-C; 3′-product (**2**): 5′-d(CTGGATTCCACTCGCC); S-link substrate (**3**): 5′-d(GGGCAT-**X**-**Y**-TGGATTCCACTCGCC) where **Y** is 5′-mercapto-2′-deoxy-C; O-link substrate (**4**): 5′-d(GGGCAT-**X**-CTGGATTCCACTCGCC); ligation template (**5**): 5′-d(AATCCAGGATGCCC)-3′-biotin. Oligonucleotides were synthesized and PAGE purified as described previously.[14]

Synthesis of 5′-Thiophosphorylated-oligo-2. 1 μmol of solid support bound, protected 5′-hydroxy-oligo-**2** was converted to the 5′-iodide by treatment with 1 mL of 0.5 M triphenoxy-methylphosphonium iodide $[(PhO)_3PCH_3][I]$ in dry DMF for 5 min, at room temp, in the dark.[43] The solid phase was then washed with 10 × 1 mL CH_2Cl_2, followed by 5 × 1 mL CH_3CN and 5 × 1 mL CH_2Cl_2, and then vaccuum-dried. The 5′-iodide was then converted to the 5′-thiophosphate by shaking the solid phase with 1 mL of aqueous 200 mM sodium thiophosphate for 72 h,[44] under N_2, at room temp, in the dark. Samples were then lyophilized, resuspended in 1 mL of concentrated NH_4OH, and deprotected at room temperature for 22 h. The NH_4OH was decanted, and the solid phase was washed with ethanol; these were combined and vaccuum-dried. The sample was then resuspended in 25 mM Na-borate (pH 9), G-10 spin column desalted, and combined with 1 volume 90% formamide/50 mM EDTA. The 5′ thiophosphorylated-oligo-**2** was purified by 16% denaturing PAGE (TBE) using authentic 5′-phosphorylated-oligo-**2** as a mobility standard. The product band was identified by UV-shadowing and excised from the gel. The purified product was then eluted from the crushed gel slice into 25 mM Na-borate (pH 9)/5 mM EDTA by freezing and then shaking at room temp for 2 h. The eluate was then decanted and concentrated to ∼60 μL using butanol and then desalted by G-10 spin column. Na-borate buffer (pH 9) was added to 10 mM for storage at −20 °C.

MALDI-TOF Analysis. Approximately 2 nmol of 5′-thiophosphorylated-oligo-**2** was dephosphorylated by treatment with 25 mM NH_4OAc (pH 5) at 37 °C for 1 h followed by G-10 spin column desalting. Untreated and NH_4OAc treated samples were concentrated to 200−300 μM and further desalted by incubating with a small portion of cation exchange resin (Bio-Rad AG50W-X8 resin, NH_4^+ form). The matrix solutions used were saturated 3-hydroxypicolinic acid in 50/50 CH_3CN/H_2O or 0.5 M trihydroxyacetophenone in ethanol, each of which was combined in a 4:1 ratio with 2.4% aqueous ammonium citrate. A 0.5 μL portion of the matrix/citrate solution was applied to the MALDI target and allowed to air-dry. A 0.5 μL portion of sample was then applied and air-dried, followed by another 0.5 μL of the matrix/citrate solution. Spectra were recorded using Bruker BiFlex II or Applied Biosystems Voyager instruments in linear negative ion mode.

Synthesis of the S-Link Substrate. 20 pmol of oligo-**1** were 5′-^{32}P-labeled using T4 polynucleotide kinase and γ-^{32}P-ATP (typically 50 μCi). The sample was then phenol/chloroform extracted, precipitated with 1% $LiClO_4$ in acetone, resuspended in 10 mM Tris-HCl (pH 7.5), and G-10 spin column desalted. 5′-^{32}P-oligo-**1** was then ligated to the 5′-thiophosphorylated-oligo-**2** under the following conditions: 50 mM Na-PIPES pH 6.7, 2 mM $MgCl_2$, 5 M DTT, 20 units of RNase inhibitor, 10 μM 5′-thiophosphorylated-oligo-**2**, 0.5 μM biotinylated oligo-**5**, 2 units of DNA ligase, in 50 μL for 2 to 3 h at 16 °C. 100 μL of avidin magnetic particles were washed with 4 × 100 μL of 100 mM NaCl/25 mM Na-PIPES (pH 6.7)/10 mM EDTA, resuspended in 50 μL of the same solution, and added to the ligation reaction. The mixture was incubated at 16 °C for 15 min with occasional agitation to allow the biotinylated duplex to bind to the solid phase avidin. The particles were then sequestered by magnetization and the supernatant decanted. The following brief washes were then applied to the particles (10 to 15 s. each): 1× (100 μL of 500 mM NaCl/100 mM Na-PIPES/10 mM EDTA), 1 × 100 μL (100 mM NaCl/25 mM Na-PIPES/10 mM EDTA), 5 × 100 μL of 5 mM Na-PIPES, 1 × 100 μL of H_2O. Finally, incubation in 10% aqueous formamide for 1 min at 37 °C liberated the desired S-link substrate (oligo-**3**) from the solid phase bound duplex. After magnetization, oligo-**3** was recovered in the supernatant, which was then G-10 spin column desalted, diluted with water (usually ∼5 volumes), and used directly in kinetic experiments.

Characterization of the S-Link Substrate. 5′-^{32}P-labeled oligos-**3** and -**4** were treated as follows: (1) 5 mM $AgNO_3$ for 10 min at room temp. AgCl was then precipitated with the addition of NaCl to 20 mM to prevent anomalous PAGE mobility in the presence of Ag^+. The sample was then centrifuged briefly and decanted. (2) 5 mM $Cd(NO_3)_2$ for 10 min at room temp. (3) 1 unit RNaseA for 10 min at 37 °C. (4) 50 mM NaOH for 10 min at 60 °C. (5) 1 μM wildtype ribozyme/5 mM $MgCl_2$/50 mM Na-PIPES (pH 7) for 10 min at room temp. All reactions were quenched by the addition of two volumes of 90% formamide/50 mM Na-PIPES (pH 6.4)/25

(39) Velikyan, I.; Acharya, S.; Trifonova, A.; Foldesi, A.; Chattopadhyaya, J. *J. Am. Chem. Soc.* **2001**, *123*, 2893–2894.
(40) Lyne, P. D.; Karplus, M. *J. Am. Chem. Soc.* **2000**, *122*, 166–167.
(41) Acharya, S.; Foldesi, A.; Chattopadhyaya, J. *J. Org. Chem.* **2003**, *68*, 1906–1910.
(42) Milligan, J. F.; Groebe, D. R.; Witherell, G. W.; Uhlenbeck, O. C. *Nucleic Acids Res.* **1987**, *15*, 8783–8798.
(43) Miller, G. P.; Kool, E. T. *Org. Lett.* **2002**, *4*, 3599–3601.
(44) Zhang, B.; Cui, Z.; Sun, L. *Org. Lett.* **2000**, *3*, 275–278.

mM EDTA/0.01% xylene cyanol/0.01% bromophenol blue. Samples were analyzed by 20% TAE denaturing PAGE (pH 6.7).

Ribozyme Kinetic Experiments. Reactions were conducted under single turnover conditions with a saturating excess of ribozyme (10 to 12.5 μM) and a trace of (<10 nM) 5′-^{32}P-labeled substrate. The standard conditions were 2 mM $MgCl_2$, 100 mM NaCl, 50 mM Na-PIPES (pH 7) at room temp (22−23 °C); other conditions are described in the text. The pH−rate profiles were conducted using Na-MES (pH 5.5 and 6), Na-PIPES (pH 6.5 and 7), Tris-HCl (pH 7.5−8.5), and Na-Borate (pH 9). Ribozymes were diluted first in buffer alone and heated to 95 °C for 2 min and then allowed to cool to room temp for ∼10 min. At this point substrate was added to ribozyme. The mixture was allowed to stand at room temp for 1 min at which point an aliquot was quenched for a zero time point. The reaction was started immediately by the addition of $MgCl_2$ and NaCl, or other metal cations as indicated in the text. Time point aliquots were quenched in four volumes of either 90% formamide/50 mM Na-PIPES (pH 6.4)/25 mM EDTA/0.01% xylene cyanol/0.01% bromophenol blue for S-link reactions or 90% formamide/50 mM EDTA/0.01% xylene cyanol/0.01% bromophenol blue for O-link reactions. All aliquots were immediately placed on powdered dry ice following addition of quench solution. The products were resolved by 20% TBE denaturing PAGE for O-link and 20% TAE[45] denaturing PAGE for S-link experiments. Samples were loaded onto running gels, with care taken to minimize the time the aliquots were thawed before gel loading. Phosphorimagery data were processed using Imagequant v5.2. Nonlinear least-squares fits were generated using Sigma Plot. Substrate cleavage data were fit to the equation: $P = P_0 + P_\infty(1 - e^{-kt})$ where P is the fraction substrate cleaved, P_0 is the initial fraction cleaved, P_∞ is the final fraction cleaved, k_{obs} is the observed first-order rate constant, and t is time. All experiments were repeated 3 to 5 times, and the results averaged; error bars correspond to standard errors.

Results

Preparation and Characterization of the S-Link Substrate. Both all-RNA[33] and embedded-ribose DNA[32] S-link substrates have been synthesized for minimal hammerhead ribozymes, and more recently, an elegant 2′-OH photodeprotection strategy was exploited to generate an S-link substrate for the HDV ribozyme.[29] In all of these cases, novel modified nucleoside phosphoramidites were prepared for solid phase synthesis of the S-link substrates. To avoid the cost and time to synthesize modified phosphoramidites, we have developed a simple ligation based method (Scheme 2) to produce radiochemical quantities of S-link substrate, suitable for use in single-turnover reactions. This strategy requires the 5′-thiophosphorylated oligo-**2** as a ligation substrate, which we have prepared by a simple solid supported synthesis.

To introduce the requisite bridging-thiophosphate at the 5′-end of oligo-**2**, the 5′-hydroxyl of protected, solid supported oligo-**2** was first converted to the 5′-iodide by brief treatment with $[(PhO)_3PCH_3]I$ in DMF.[43] The 5′-thiophosphate moiety (bonded to the 5′-carbon via sulfur) was then introduced by treatment with aqueous Na_3SPO_3.[44] Following NH_4OH deprotection, PAGE purification, and desalting, the yield of the desired product was quite low (ca. 10%); however, a standard 1 μmol scale oligonucleotide synthesis furnished more than ample quantities for our purposes. 5′-Thiophosphorylated-oligo-**2** was maintained at pH 9, where it is relatively stable to hydrolysis;[46] its identity was confirmed by MALDI-TOF mass spectrometry (see Supporting Information). Also, the 5′-thiophosphate was quickly and quantitatively hydrolyzed at pH 5 to yield 5′-thiol-oligo-**2**, proving that the thiophosphate is bonded to the 5′-carbon exclusively via sulfur, not oxygen (see Supporting Information).

To produce the full length S-link substrate, 5′-^{32}P-labeled oligo-**1** and 5′-thiophosphorylated-oligo-**2** were annealed to biotinylated template oligo-**5** and joined using DNA ligase (Scheme 2). The resulting biotinylated duplex was bound to streptavidin magnetic particles. Low salt washes released unreacted oligos-**1** and -**2** from the solid phase bound template (oligo-**5**), as just 7 base pairs are formed between oligo-**5** and each of oligos-**1** and -**2**. Finally, the desired S-link substrate (oligo-**3**), more strongly bound to the template by 14 base pairs, was liberated from the solid phase under mildly denaturing conditions. Following the work of Kuimelis and McLaughlin,[45,47] the S-link substrate was maintained at pH 6.7 (Na-PIPES) in the absence of M^{2+} whenever possible during preparation and purification, as the bridging phosphorothioate linkage is relatively stable under these conditions. Accordingly, ribozyme reactions were quenched at pH 6.7, and the samples were analyzed using PAGE gels cast in TAE/urea buffer (pH 6.7), as opposed to TBE/urea buffer (pH 8.3). Mg^{2+} is required in the ligation buffer but was not detrimental, as S-link substrates are particularly stable in the context of a DNA duplex.[45]

The constitution and purity of the S-link substrate were verified by comparison of its properties to those of the native O-link substrate (Figure 2). As expected, the 5′-^{32}P-labeled S-link and O-link substrates were indistinguishable by denaturing PAGE (lanes 1 and 2), as were their 5′-^{32}P-labeled-5′-cleavage products (lanes 3−6). Both substrates were efficiently cleaved by the hammerhead ribozyme (lanes 3 and 4) and Ribonuclease A (lanes 5 and 6). Cleavage of the bridging-thio linkage in RNA is known to be promoted by soft metal cations, whereas cleavage of native RNA is not;[29,45,47] accordingly, brief treatment with Cd^{2+} caused rapid cleavage of the S-link substrate, but not the O-link substrate (lanes 9 and 10). Most importantly, brief treatment with NaOH (60 °C) or Ag^+ caused quantitative cleavage of the S-link substrate but had little or no effect on the O-link substrate (lanes 7, 8, 11, and 12). These results demonstrate that the S-link substrate synthesized via our method is not detectably contaminated with any native or other undesired RNA linkage.

Our ligation procedure yielded consistently pure S-link substrate (usually >97% pure) in 2−3 h without the need to synthesize modified phosphoramidites. This method may be useful especially for incorporation of the bridging phosphorothioate linkage in the middle of longer sequences; in such cases, incorporation of the bridging phosphorothioate by solid phase synthesis is difficult due to its sensitivity to the conditions used in subsequent nucleotide coupling cycles and deprotection.

Hammerhead Cleavage of O-Link and S-Link Substrates. Hammerhead cleavage of the S-link and O-link substrates was compared for several sequence mutations and discrete chemical modifications to locate ribozyme functional groups involved specifically in general acid catalysis. The standard conditions (2 mM $MgCl_2$, 100 mM NaCl, 50 mM Na-PIPES pH 7) were chosen such that all cleavage reactions could be monitored by

(45) Kuimelis, R. G.; McLaughlin, L. W. *Biorg. Med. Chem.* **1997**, *5*, 1051–1061.
(46) Dittmer, D. C.; Ramsay, O. B.; Spalding, R. E. *J. Org. Chem.* **1963**, *28*, 1273–1278.
(47) Kuimelis, R. G.; McLaughlin, L. W. *Biochemistry* **1996**, *35*, 5308–5317.

Scheme 2. Ligation Based Synthesis of the S-Link Substrate

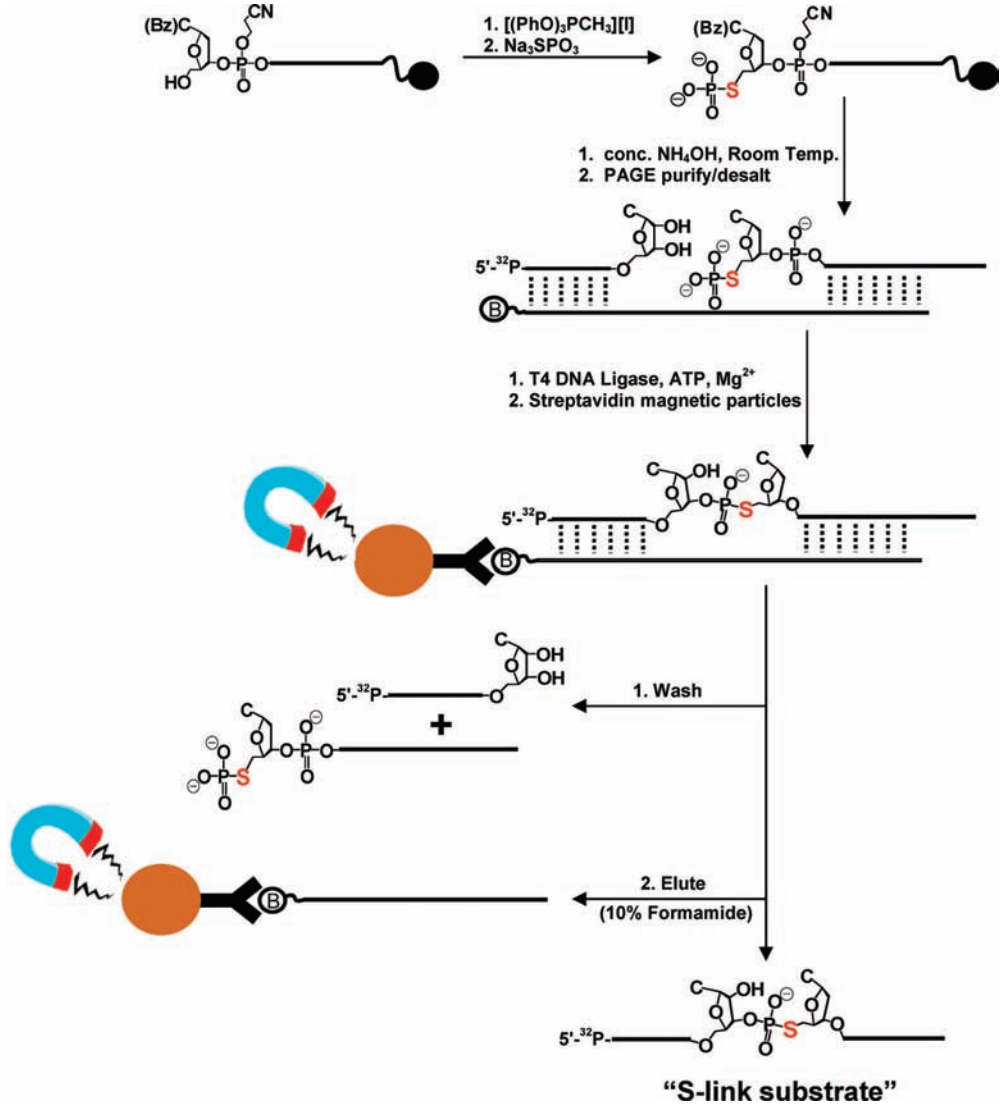

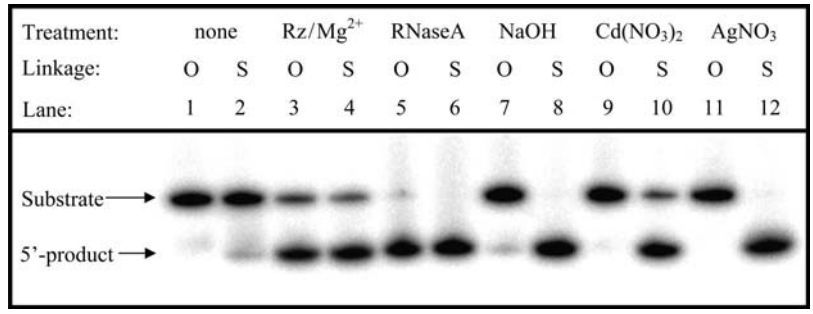

Figure 2. Comparison of the properties of the O-link and S-link substrates (5′-^{32}P-labeled) and their 5′-cleavage products. Lanes 1 and 2: no treatment. Lanes 3 and 4: 1 μM wildtype ribozyme, 2 mM $MgCl_2$, 50 mM Na-PIPES pH 7 for 10 min. Lanes 5 and 6: 1 unit RNaseA, 50 mM Na-PIPES pH 7 for 10 min. Lanes 7 and 8: 50 mM NaOH 60 °C for 10 min. Lanes 9 and 10: 5 mM $Cd(NO_3)_2$ for 10 min. Lanes 11 and 12: 5 mM $AgNO_3$ for 10 min. Samples were analyzed by 20% TAE denaturing PAGE.

manually quenched kinetics experiments. In several cases,[48] biphasic kinetics were observed when longer time points were included; in these cases, the reported rate constants represent the faster cleavage phase and were obtained by fitting earlier time points. Such biphasic kinetics have been reported previously for extended hammerhead ribozymes, including the *S. mansoni*.[49,50] A reported k_{obs} value of <0.00001 min^{-1} indicates

(48) Biphasic cleavage kinetics were more apparent in the case of the S-link substrate. See Figures S3 and S4 in the Supporting Information for further explanation.

(49) Kim, N.-K.; Murali, A.; DeRose, V. J. *J. Am. Chem. Soc.* **2005**, *127*, 14134–14135.

(50) Canny, M. D.; Jucker, F. M.; Pardi, A. *Biochemistry* **2007**, *46*, 3826–3834.

Table 1. First-Order Rate Constants for Single Turnover Cleavage of O-Link and S-Link Substrates by the *S. mansoni* Hammerhead Ribozymes[a]

ribozyme	k_O (min^{-1})	k_S (min^{-1})	k_S/k_O	k_{catS}/k_{uncatS}	k_{catO}/k_{uncatO}
WT	0.86	3.2	3.7	1.1×10^4	8.6×10^7
2′-OMe-G8[b]	0.00013	1.9	14600	6.6×10^3	1.3×10^4
dG8[c]	0.0025	4.6	1840	1.6×10^4	2.5×10^5
dA6[c]	0.81	3.3	4.1	1.1×10^4	8.1×10^7
dG5[c]	0.00079	0.33	417	1.1×10^3	7.9×10^4
A14G	<0.00001	0.02	>2000	6.9×10^1	$<1.0 \times 10^3$
G12c7[d]	0.014	0.50	35	1.7×10^3	1.4×10^6
G12A	<0.00001	0.094	>9400	3.2×10^2	$<1.0 \times 10^3$
G12U	<0.00001	0.058	>5800	2.0×10^2	$<1.0 \times 10^3$
A9U	0.0076	4.0	526	1.4×10^4	7.6×10^5
A9c7[e]	0.0017	3.4	2000	1.2×10^4	1.7×10^5
G8A	0.00008	0.14	1750	4.8×10^2	8.0×10^3
A6U	0.00005	0.16	3200	5.5×10^2	5.0×10^3
BP[f]	0.030	1.1	36	3.8×10^3	3.0×10^6
background	$\sim 1 \times 10^{-8}$[g]	0.00029	~29000	1	1

[a] All reactions contained 2 mM $MgCl_2$, 100 mM NaCl, 50 mM Na-PIPES pH 7. [b] 2′-O-methyl. [c] 2′-deoxyribo. [d] 7-deaza-guanosine. [e] 7-deaza-adenosine. [f] BP or "Base Paired" indicates a ribozyme sequence altered in order to disrupt the tertiary interaction highlighted in Figure 1. In the BP mutant, the bulge between the substrate and ribozyme strands was replaced with a continuously base paired sequence (see Supporting Information). [g] Rate constant estimated based on data in ref 52.

that substrate cleavage was too slow to quantify reliably (reactions were monitored up to 100 h).

Most of the mutants and chemical variants chosen have been characterized for minimal hammerheads in the context of O-link substrates but, in most cases, not for extended hammerheads. The effects of ribozyme mutations on O-link substrate cleavage reported here for the *S. mansoni* hammerhead parallel those for the minimal hammerheads;[7] furthermore, we find that an embedded ribose DNA substrate is cleaved efficiently by the *S. mansoni* hammerhead as it is by minimal hammerheads.[32,51] Table 1 presents the observed rate constants for single turnover cleavage of the S-link and O-link substrates by the *S. mansoni* hammerhead and various mutants, as well as for background substrate cleavage. Cleavage of S-link and O-link substrates was also compared in the presence of various metal cations at pH 7 for the wildtype and the dG8 and 2′-OMe-G8 variants (Table 2). Large k_S/k_O values indicate that the chosen mutant or reaction conditions impair general acid catalysis in particular.[29,36,37] Thus our data suggest that both an M^{2+} cofactor and the G8 2′-OH play crucial roles in general acid catalysis, although several other residues also appear to be important in facilitating general acid catalysis (see Discussion).

pH−Rate Profiles. We conducted pK_a perturbation experiments to confirm the role of both the G8 2′-OH and Mg^{2+} in general acid catalysis and to probe the mechanism in more detail. General acid pK_a perturbation was achieved in two ways: (1) by replacement of Mg^{2+} with Cd^{2+} and (2) by chemical modification of the G8 2′-OH. These effects are revealed in the pH−rate profiles for O-link substrate cleavage by the wildtype, dG8, and 2′-OMe-G8 hammerheads in both Mg^{2+} and Cd^{2+} containing solutions (Figure 3). The data were fit to a general acid/base catalysis model,[53] and the kinetic pK_a's generated are presented in Table 3. Given that general base catalysis by G12 (with pK_a ~8) is suggested convincingly by crystallographic,[11−13] computational,[17,18] and functional evidence,[14,15] the kinetic pK_a closest to 8 was assigned to the general base and the other to the general acid (see Discussion). In all cases, except for the wildtype ribozyme in the presence of Cd^{2+}, one of the titrations clearly demonstrated a pK_a near 8 within the standard error limits. Rate constants determined in the presence of Cd^{2+} at pH > 8 are likely unreliable due to $Cd(OH)_2$ precipitation; therefore, these data were not included in the fits.[28]

Table 2. First-Order Rate Constants for Single Turnover O-Link and S-Link Substrate Cleavage by the Wildtype, 2′-Deoxy-G8, and 2′-O-Methyl-G8 in the Presence of Various Metal Cations[a]

conditions	ribozyme	k_O (min^{-1})	k_S (min^{-1})	k_S/k_O
2 mM Mg^{2+} + 100 mM NaCl	WT	0.86	3.2	3.7
	dG8	0.0025	4.6	1840
	2′-OMe-G8	0.00013	1.9	14600
0.2 mM Mn^{2+} + 100 mM NaCl	WT	1.2	2.5	2.1
	dG8	0.0070	2.9	414
	2′-OMe-G8	0.0028	0.35	125
1 mM Cd^{2+} + 100 mM NaCl	WT	2.2	2.7	1.2
	dG8	0.057	2.6	46
	2′-OMe-G8	0.0018	3.3	1830
100 mM NaCl[b]	WT	<0.00001	2.7	>270000
	dG8	<0.00001	1.0	>100000
	2′-OMe-G8	<0.00001	0.17	>17000
100 mM LiCl[b]	WT	0.00017	2.5	14700
	dG8	<0.00001	2.3	>230000
	2′-OMe-G8	<0.00001	0.70	>70000

[a] All reactions contained 50 mM Na-PIPES pH 7. [b] 5 mM EDTA was included in NaCl and LiCl containing reactions.

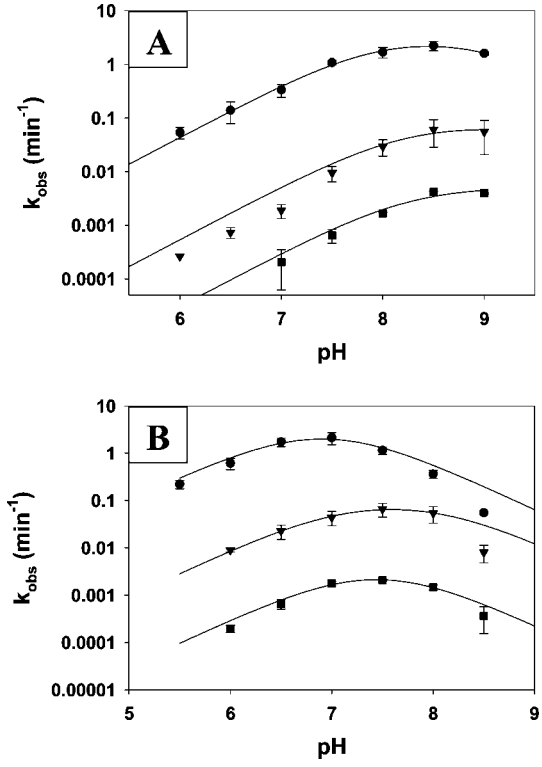

Figure 3. Kinetic pH−rate profiles for O-link substrate cleavage by the (●) wildtype, (▼) 2′-deoxy-G8, and (■) 2′-OMe-G8 *S. mansoni* hammerhead ribozymes in the presence of (A) 1 mM Mg^{2+} and (B) 1 mM Cd^{2+}. All reactions contained 100 mM NaCl and 50 mM buffer. The data were fit to a general acid/base catalysis model: $k_{obs} = k_{max}/(1 + 10^{pK_{a1}-pH} + 10^{pH-pK_{a2}} + 10^{pK_{a1}-pK_{a2}})$.[53] Data for Cd^{2+} containing reactions at pH > 8 are included in the plot but were omitted from the fits as 1 mM Cd^{2+} is prone to precipitation above pH 8. Error bars indicate standard errors in the data points.

(51) Yang, J.-H.; Perreault, J.-P.; Labuda, D.; Usman, N.; Cedergren, R. *Biochemistry* **1990**, *29*, 11156–11160.
(52) Soukup, G. A.; Breaker, R. R. *RNA* **1999**, *5*, 1308–1325.

Table 3. pK_a Values Determined from the pH−Rate Profile Data As Detailed in Figure 3[a]

ribozyme	M^{2+}	general base pK_a	general acid pK_a
WT	Mg^{2+}	7.9 ± 0.2	9.0 ± 0.2
dG8	Mg^{2+}	8.2 ± 0.8	>9[b]
2′-OMe-G8	Mg^{2+}	8.2 ± 0.2	>9[b]
WT	Cd^{2+}	7.0 ± 0.6	6.7 ± 0.4
dG8	Cd^{2+}	8.1 ± 0.5	7.1 ± 0.4
2′-OMe-G8	Cd^{2+}	7.5 ± 0.6	7.4 ± 0.5

[a] All reactions contained 1 mM M^{2+}, 100 mM NaCl, 50 mM buffer. The rationale for the assignment of pK_a values to the general acid or base titrations is given in the text. Standard error limits generated by fitting the pH−rate profile data are given. [b] These pK_a values could not be determined with acceptable precision as the corresponding titrations are outside of the observable pH range. Based on the data shown in Figure 3A, these pK_a values appear, qualitatively, to be significantly higher than 9.

Table 3 shows that replacement of Mg^{2+} with Cd^{2+} drastically lowers the general acid pK_a by ∼2 units. In addition, the general acid pK_a appears to increase slightly when proton transfer from the G8 2′OH is abolished in the dG8 and 2′-OMe-G8 variants (Figure 3B). The general acid titrations for the dG8 and 2′-OMe hammerheads in the presence of Mg^{2+} fell outside the observable range (pK_a >9); thus these pK_a values could not be determined with high precision. Nevertheless it is clear, qualitatively, that the general acid pK_a is also perturbed upward for the dG8 and 2′-OMe-G8 variants in the presence of Mg^{2+} (Figure 3A), although caution must be exercised in interpreting data so close to the onset of alkaline denaturation (at pH ∼9).

Discussion

Hammerhead Cleavage of O-Link and S-Link Substrates. Previously, others have used S-link substrates to investigate minimal hammerhead ribozyme catalysis;[32,33,47] however, the role of ribozyme functional groups in general acid catalysis was not investigated. These studies demonstrated that minimal hammerhead cleavage of S-link substrates was not significantly enhanced in the presence of soft, thiophilic metal cations. This finding strongly suggested that the 5′-leaving group is not stabilized by direct coordination to a Lewis acidic metal cation.[32,33,47] Nevertheless, it was cautioned that a two metal ion mechanism, involving both M^{2+}-mediated Lewis acid and base catalysis (Scheme 3A), could also be consistent with the apparent lack of activation of S-link cleavage by soft metal cations.[54−56] Our results confirm that Mn^{2+} and Cd^{2+} do not significantly enhance cleavage of the S-link substrate by the *S. mansoni* hammerhead relative to Mg^{2+} or even monovalent cations alone (Table 2). Given that the G12 nucleobase is convincingly implicated in general base catalysis (not an M^{2+} cofactor),[11−15,17,18] it appears most likely that a two-metal ion mechanism invoking both M^{2+}-mediated Lewis acid and general base catalysis is not operative.

The largest k_S/k_O values, which indicate the most dramatic restoration of ribozyme activity by the S-link substrate, are manifested in the absence of divalent metal cations (Table 2). This indicates that omission of an M^{2+} cofactor specifically disrupts general acid catalysis. Moreover, the fact that the absence of an M^{2+} cofactor does not significantly affect S-link cleavage by the *S. mansoni* hammerhead suggests that an M^{2+} cofactor does not play any crucial role in catalysis other than participation in general acid catalysis. In contrast, cleavage of an S-link substrate by a minimal hammerhead in 0.5 M NaCl was reportedly undetectable.[32] This discrepancy suggests that M^{2+} binding is required to stabilize the active ribozyme conformation in the minimal hammerhead, whereas the *S. mansoni* hammerhead does not require such M^{2+}-mediated structural stabilization, likely due to its additional tertiary stabilization motif.

Consistent with its proximity to the leaving group in the *S. mansoni* crystal structure, the G8 2′OH also appears to be crucial for general acid catalysis, as indicated by the large k_S/k_O values observed upon modification of this functional group (in the 2′-dG8 and 2′-OMe-G8 variants) (Table 1). Analogous experiments on the HDV ribozyme gave unambiguous results, with large k_S/k_O values observed only for modifications of the N3 position of C75 (the putative general acid in the HDV ribozyme).[29] In contrast, we observed significant k_S/k_O values for modification of several hammerhead ribozyme residues in addition to the putative G8 2′OH general acid. Such an S-link rescue of multiple active site mutants has been observed for a phospholipase enzyme, which catalyzes a similar intramolecular phosphodiester transesterification.[37] Based on previous crystal structure data for this enzyme, the authors concluded that S-link rescue of mutations to residues other than the putative general acid resulted from disruption of hydrogen bonds necessary for proper general acid placement. In the hammerhead ribozyme, the crystallographically observed[11−13] G8:C3 canonical base pair has been predicted computationally[57] to be crucial for proper positioning of the G8 2′OH to engage in proton transfer to the oxygen leaving group. The significant degree of S-link rescue observed for the G8A mutant is consistent with this hypothesis. In addition, significant S-link rescue of the A9U and A9−7deaza ($A9c^7$) variants suggests that the G12:A9 sheared pair, observed in the *S. mansoni* crystal structure (Scheme 1),[11−13] is also important for productive placement of the G8 2′OH general acid.

Large k_S/k_O values were also observed for mutations to the putative hammerhead general base (G12). Again, it is not surprising that disruption of the G12:A9 interaction in the G12A and G12U mutants should affect proper placement of the G8 2′OH and/or an M^{2+} cofactor bound to the A9-phosphate. However, Scott and co-workers have recently shown that a prereactive state crystal structure of the G12A mutant remains largely unchanged relative to wildtype,[13] although disruption of the ribozyme conformation at or near the transition state cannot be excluded.

While large k_S/k_O ratios were observed for each of the A6U, G12A, G12U, and A14G mutants, it should also be noted that both S-link and O-link cleavage are enhanced by a factor of less than 10^3 relative to background cleavage in these cases. Soukup and Breaker have reported similar enhancement of background RNA cleavage due to geometrical constraints imposed by secondary and tertiary structures.[52] Kuimelis and McLaughlin showed that background S-link cleavage is also dependent on the structural context.[45] Similarly, structural constraints imposed by ribozyme binding could favor the reactive in-line attack geometry and could account for the relatively small enhancement of both S-link and O-link cleavage over their respective background cleavage rates for the A6U, G12A, G12U, and A14G mutants. Thus the large k_S/k_O values

(53) Bevilacqua, P. C. *Biochemistry* **2003**, *42*, 2259–2265.
(54) Pontius, B. W.; Lott, W. B.; von Hippel, P. H. *Proc. Natl. Acad. Sci. U.S.A.* **1997**, *94*, 2290–2294.
(55) Zhou, D.-M.; Zhang, L.-H.; Taira, K. *Proc. Natl. Acad. Sci. U.S.A.* **1997**, *94*, 14343–14348.
(56) Leclerc, F.; Karplus, M. *J. Phys. Chem. B* **2006**, *110*, 3395–3409.
(57) Lee, T.-S.; York, D. M. *J. Am. Chem. Soc.* **2008**, *130*, 7168–7169.

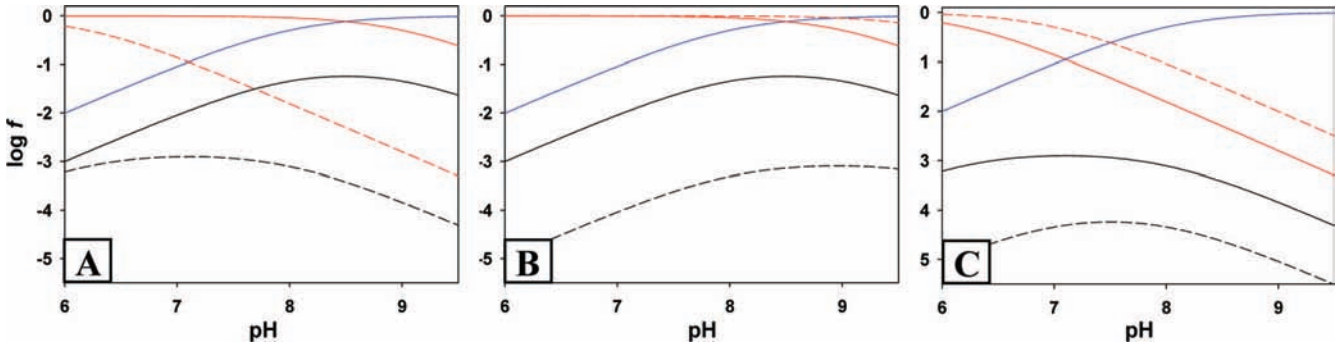

Figure 4. Simulation of the effects on the pH−rate profile for O-link substrate cleavage caused by perturbation of the general acid pK_a. The general base titration, given by $f = 1/(1 + 10^{pK_{a1}-pH})$, is blue. The general acid titration, given by $f = 1/(1 + 10^{pH-pK_{a2}})$, is red. The fraction of ribozyme in the fully active protonation state, given by $f = f_{max}/(1 + 10^{pK_{a1}-pH} + 10^{pH-pK_{a2}} + 10^{pK_{a1}-pK_{a2}})$, is black. (A) Substitution of Cd^{2+} (---) for Mg^{2+} (—) dramatically lowers the pK_a of the general acid. (B) Presumed substitution of a Mg^{2+}-bound water ligand for the G8 2′OH slightly increases the pK_a of the general acid in the dG8 variant (---) relative to wildtype (—). (C) The dG8 modification (---) similarly raises the general acid pK_a relative to wildtype (—) in the presence of Cd^{2+}. The general base titration is constant in all cases (pK_a set to 8). For clarity, f_{max} was set to 0.1 for wildtype and 0.001 for dG8.

Scheme 3. Possible Mechanisms of General Acid Catalysis Involving Both the G8 2′OH and a Mg^{2+} Cofactor

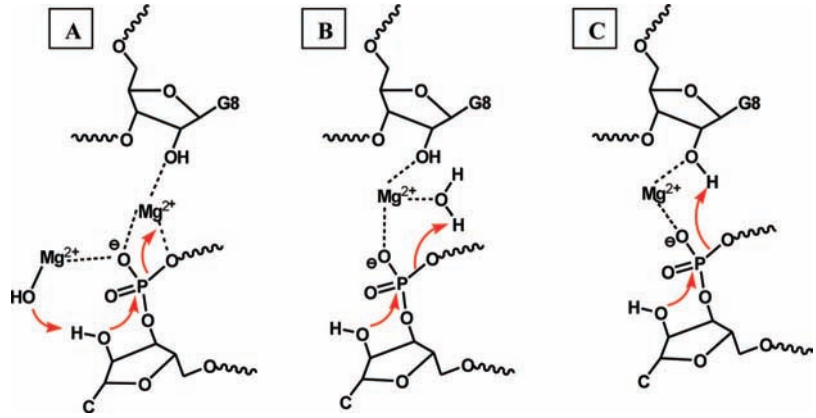

observed for these mutants may simply reflect more facile background S-link cleavage in the context of inactive ribozyme−substrate complexes.

pH−Rate Profiles. The S-link cleavage data indicate that both an M^{2+} cofactor and the G8 2′OH play important roles in facilitating proton transfer to the leaving group. These data could be consistent with a general acid mechanism where the G8 2′OH acts simply as a ligand to ensure proper placement of a hydrated M^{2+} cofactor. In this case, an M^{2+}-bound water ligand could serve directly as the general acid (Scheme 3B). Alternatively, the G8 2′OH could act as the general acid, where M^{2+} coordination could serve to lower its pK_a and facilitate proton transfer to the leaving group (Scheme 3C). To discriminate between these two closely related mechanisms, and to validate the S-link cleavage data, we examined the effects of M^{2+} substitution and G8 2′OH modification on the pH−rate profiles for O-link substrate cleavage.

In general, the assignment of kinetic pK_a's to the general acid or general base is inherently ambiguous; however, this ambiguity can be overcome with the benefit of S-link cleavage data and guidance from crystal structures.[53] Das and Piccirilli provide an outstanding example of such reasoning in their study of general acid catalysis in the HDV ribozyme.[29] These authors attributed pH−rate profile changes for O-link substrate cleavage to general acid pK_a perturbation in the case of a C75(6-azaC)[58] substitution, based on the large k_S/k_O values observed specifically for C75 variants, which implicate this residue in general acid catalysis. Considering the *S. mansoni* crystal structures[11−13] and our S-link cleavage results which implicate both the G8 2′OH and an M^{2+} cofactor in general acid catalysis, we attribute pH−rate profile changes caused by M^{2+} or G8 2′OH alteration to general acid pK_a perturbation. Consistent with this interpretation, a kinetic pK_a close to 8 was determined for almost all variants under all conditions examined, which was taken to reflect invariant general base catalysis by G12.

For each of the wildtype, dG8, and 2′OMe-G8 hammerhead variants, replacement of Mg^{2+} with Cd^{2+} lowers the general acid pK_a (Table 3 and Figure 3); this is exemplified by the simulations shown in Figure 4A. This result is consistent with the pK_a difference between the respective metal−aqua complexes (the pK_a of $Mg(H_2O)_6^{2+}$ is 11.4 whereas the pK_a of $Cd(H_2O)_6^{2+}$ is 8.0)[28] and confirms M^{2+} involvement in general acid catalysis as suggested by the S-link cleavage data; similar results have also been reported for cleavage of an all-RNA substrate by a different extended hammerhead (RzB).[28] However, these data cannot resolve the question of whether an M^{2+}-coordinated water molecule (Scheme 3B) or an M^{2+}-coordinated

(58) 6-Aza-cytosine has a lower N3-conjugate acid pK_a than natural cytosine; thus the C75(6-azaC) substitution was observed to perturb the general acid pK_a downward for O-link substrate cleavage by the HDV ribozyme. See: Das, S. R.; Piccirilli, J. A. *Nat. Chem. Biol.* **2005**, *1*, 45–52.

(59) Sigel, R. K. O.; Pyle, A. M. *Chem. Rev.* **2007**, *107*, 97–113.

Scheme 4. Possible General Acid Catalysis Mechanisms for (A) Wildtype and (B) dG8 Hammerhead Ribozymes

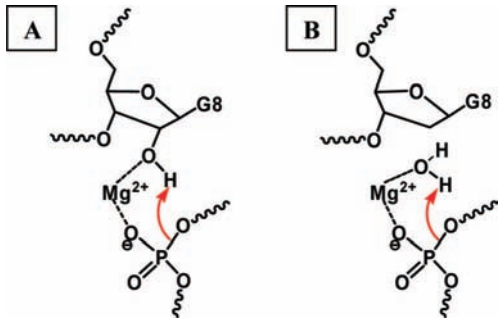

G8 2′OH (Scheme 3C) transfers a proton to the 5′-oxygen leaving group.

To discriminate between the mechanisms depicted in Scheme 3B and C, the pH−rate profiles for O-link cleavage by the wildtype, dG8, and 2′OMe-G8 hammerheads were compared in the presence of Mg^{2+} or Cd^{2+}. In the presence of either M^{2+}, the general acid pK_a value appears to be shifted higher for both the dG8 and 2′OMe-G8 variants relative to wildtype (Figure 3). This effect is particularly clear in the presence of Cd^{2+} and appears to hold true in Mg^{2+}, although one must be cautious in drawing conclusions from pH effects so close to the onset of general alkaline denaturation (at pH $\sim$ 9). We propose that this upward shift in the general acid pK_a signals that an M^{2+}-bound water ligand assumes the task of transferring a proton to the leaving group when the G8 2′OH is ablated to prevent proton transfer (Scheme 4). This interpretation is qualitatively consistent with the pK_a difference between water (pK_a = 15.7) and an RNA 2′OH (experimental pK_a values for model compounds range from $\sim$12.5 to 13.5,[39,41] although theoretical predictions range as high as 14.9[40]). It is reasonable that this pK_a difference should be reflected, qualitatively at least,[55] in comparing the general acid pK_a's exhibited by M^{2+}-bound water (in the dG8 and 2′OMe-G8 variants) versus the M^{2+}-bound G8 2′OH (in the wildtype); this effect is illustrated by simulation in Figures 4B and 4C. This hypothesis is also consistent with the more severe impairment of O-link cleavage activity for the G8 2′OMe versus the dG8 variant; that is, the G8 2′OMe variant likely presents a steric impediment to proton transfer from M^{2+}-bound water to the 5′-oxygen leaving group, whereas the dG8 variant does not.

Conclusions

In summary, our comparison of hammerhead mediated O-link and S-link substrate cleavage suggests the synergistic involvement of the G8 2′OH and an M^{2+} cofactor in general acid catalysis in the hammerhead ribozyme. These data, coupled with the general acid pK_a perturbation observed for both M^{2+} substitution and G8 2′OH modification, provide compelling evidence to support the general acid catalysis mechanism depicted in Scheme 3C. The S-link cleavage data also reveal the importance, specifically for general acid catalysis, of new structural interactions uncovered in the *S. mansoni* crystal structure (namely the G8:C3 base pair and the G12:A9 sheared pair).[11−13] Our study provides much needed functional interrogation of the newly proposed catalytic mechanism for the hammerhead ribozyme and complements the recent crystallographic and computational advances.[11−13,17,18] In a more general sense, our findings highlight how M^{2+} coordination of RNA functional groups can serve to modulate their pK_a and improve their ability to engage in general acid catalysis at physiological pH.[59]

Acknowledgment. We thank Profs. Subha R. Das, Andrew J. Bennett, and Stephen G. Withers for helpful discussions. We also thank Suzanne Perry at the UBC Laboratory of Molecular Biophysics for obtaining MALDI spectra. This work was funded by NSERC and CIHR. Salary support was provided by NSERC CGS-D and Gladys Estella Laird fellowships (J.M.T.) and a Michael Smith Foundation Senior Career Award (D.M.P.).

Supporting Information Available: MALDI-TOF spectra, kinetics plots, and secondary structure representations of wildtype and base paired *S. mansoni* hammerhead ribozymes. This material is available free of charge via the Internet at http://pubs.acs.org.

JA807790E